

# Activation of TREK-1 Potassium Channel Improved Cognitive Deficits in Alzheimer's Disease Model Mice by Modulation of Glutamate Metabolic Pathway

Fang Li (✉ [fli2019@lzu.edu.cn](mailto:fli2019@lzu.edu.cn))

LZU Lanzhou University <https://orcid.org/0000-0001-5398-6158>

Shu ning Zhou

LZU: Lanzhou University

Xin Zeng

LZU Lanzhou University

Rui Yang

Lanzhou Hospital of Traditional Chinese Medicine

Xue Xi Wang

Lanzhou University

Bin Meng

Lanzhou University Second Hospital

Wei lin Pei

Lanzhou University Second Hospital

Li Lu

Lanzhou University <https://orcid.org/0000-0002-2224-6963>

---

## Research Article

**Keywords:** Alzheimer's disease, cognitive deficits, TREK-1, Glutamate metabolic pathways, SAMP8

**Posted Date:** March 10th, 2021

**DOI:** <https://doi.org/10.21203/rs.3.rs-258734/v1>

**License:**  This work is licensed under a Creative Commons Attribution 4.0 International License.

[Read Full License](#)

---

# Abstract

Alzheimer's disease (AD) is a progressive neurodegenerative disease characterized by cognitive dysfunction. Glutamate (Glu) metabolism pathway mediated neurotoxicity is one of main factors causing memory impairment in AD. TWIK-related potassium channel-1 (TREK-1) exerts protective effect in brain ischemia, but the role of it in AD is unknown. In this study, the SAMP8 mice were used as an AD model, the age-matched SAMR1 mice as a control, we investigated the change trend of TREK-1 channel as well as AD related molecules in brains of SAMP8 mice and showed the expression levels of TREK-1 compensatory arose before 3 months of age, then began to decline. Meanwhile the levels of Tau and Glu increased with age while Ach level decreased over age. Next, using  $\alpha$ -Linolenic acid (ALA) as an activator of TREK-1 channel, we showed that activation of TREK-1 channel improved the learning and memory deficits of SAMP8 mice aged in 6 months. Furthermore, we explored the possible mechanisms and found that the levels of molecules were closely related to the glutamate metabolism pathway. After the activation of TREK-1 channel, the damaged neurons and astrocyte were rescued, the levels of Glu and NMDAR were down-regulated, while the level of GLT-1 was up-regulated. These findings suggested that TREK-1 played the crucial role in the pathological progression of AD and activation of TREK-1 channel improved the cognitive deficits in SAMP8 mice which is mediated by Glu metabolism pathway. The TREK-1 potassium channel may be expected to be a new potential therapeutic target for AD.

## Introduction

Alzheimer's disease (AD) was defined as a progressive neurodegenerative syndrome characterized by a gradual decline in learning and memory function (Goedert et al. 2006). Memory loss, skill impairment, incapacity for decision making and discernment, decline of visuospatial function and changes in personality and behavior were some of the main clinical manifestation of the disease (Tom et al. 2015).

The accumulation of insoluble A $\beta$  oligomer and hyperphosphorylated Tau (pTau) in the brain is the major pathogenic factors for neurodegeneration in AD (Jeong. 2017). The central cholinergic system is also closely associated with the process of AD (Knox. 2016). Endogenous acetylcholine (Ach) is important for modulation of acquisition (Blokland et al. 1992), encoding (Winters et al. 2005), consolidation (Power et al. 2003), reconsolidation (Boccia et al. 2004), extinction (Boccia et al. 2009) and retrieval (Boccia et al. 2003) of memory. Severe loss of cholinergic neurons in AD is the cause of memory and attention deficits (Ferreira-Vieira et al. 2016), whereas enhancing the function of cholinergic neurons and synapses improve cognitive processes (Sofroniew et al. 2010).

Similarly, glutamate (Glu), as the most considerable excitatory neurotransmitter in central nervous system, played an important role in memory, neuronal development and synaptic plasticity (Ferraguti et al. 2008 ; Nakanishi et al. 1994). It has been found that the decrease of intelligence in AD patients may be due to the abnormality of glutamatergic neurotransmitter system (Riederer et al. 2006). Large amount of Glu accumulation mediated neurotoxic reactions and over activation of its receptors, leading to denature and necrosis of the neurons (Nakanishi et al. 1994). Among the glutamate receptors, the major neurotoxic

receptor is glutamatergic N-methyl-D-aspartate receptor (NMDAR) that is most densely distributed in the cerebral cortex and hippocampus (Danysz et al. 1988 ; Morris. 1989). NMDAR mediated delayed neuronal injury is one of the important mechanisms of learning and memory dysfunction and neuronal degeneration in AD (Revett et al. 2013 ; Shankar et al. 2007). The glutamate transporter-1 (GLT-1) is another important mechanism for keeping homeostasis of Glu content in brain by uptaking excessive extracellular glutamate into cells. Under pathological conditions, GLT-1 reduces the uptake, and even reverses its function by releasing the Glu out of the cells, leading to the aggravation of cytotoxic effect of Glu (Yi et al. 2005). It has been confirmed that the gradual decline of GLT-1 expression levels accompanied with weakening of Glu uptake function over ages in AD patients. The loss of GLT-1 induced early cognitive dysfunction in mice (Meeker et al. 2015).

TWIK related potassium channel TREK-1 is a two-pore-domain background potassium channel expressed throughout the central nervous system, especially in the cortex, hippocampus, hypothalamus, and basal ganglia, et.al (Chapman et al. 2000 ; Hervieu et al. 2001). The TREK-1 channel modulates neuronal excitability (Vivier et al. 2016) by regulating membrane potential, is activated by high body temperature, low pH, membrane stretch, and polyunsaturated fatty acids (PUFAs) such as  $\alpha$ -Linolenic acid (ALA), arachidonic acid (AA) (Yarishkin et al. 2018). Studies in recent years have demonstrated that TREK-1 potassium channels have neuroprotective effects in a variety of central nervous system diseases, such as ischemia(Wang et al. 2018), epilepsy, inflammation, anesthesia, and pain (Djillani et al. 2019 ; Honoré. 2007). Neuroprotection of PUFAs was closely involved in TREK-1 channels, for example, TREK-1<sup>-/-</sup> mice display an increased sensitivity to ischemia and (Heurteaux et al. 2004) neuroprotection disappear after ALA treatment (Liu et al. 2014). Through activation of TREK-1, ALA hyperpolarizes the resting membrane potential of astrocytes and up-regulates the decreased of GLT-1 protein level induced by focal ischemia (Lu et al. 2017). Besides, the neuroprotection of volatile anesthetics is mediated by TREK-1 and further concerned with the inhibition of NMDAR (Bittner et al. 2013). There seems to be a link between TREK-1 channel and Glu regulation based on clues above.

Although it is now clear that TREK-1 play a role in neuroprotection, the role of TREK-1 in Alzheimer's disease remains unknown. In this study, we were wonder whether TREK-1 potassium channel involved in the pathological process of AD. After activation of TREK-1, could the learning and memory deficits of AD be improved? If so, what the possible underlying mechanisms was. Senescence accelerated mice P8 (SAMP8) whose pathological changes are similar with those of human AD, is characterized by early rapid aging accompanied by significant learning and memory dysfunction (Akiguchi et al. 2017), as well abnormal deposition of A $\beta$ , hyperphosphorylation of tau protein and acetylcholine deficiency. Therefore, SAMP8 mice were used as the model of AD and the matched senescence accelerated resistant-1 (SAMR1) mice were used as the control. We firstly observed the expression changes of Tau, Ach and TREK-1 in different ages of SAMP8 mice. Next, ALA was selected as an activator of TREK-1 channel, we investigated the influences of the TREK-1 on learning and memory abilities in SAMP8 mice aged 6 months. Furthermore, the probable mechanisms related to regulation of the glutamate metabolic pathway were also elucidated.

## Methods

### Animals and experimental design

Male senescence accelerated mouse Prone 8 (SAMP8) mice and senescence accelerated mouse resistant 1 (SAMR1) mice aged 1/3/6/9 months were provided by Beijing HFK Bioscience Co., Ltd. (Permit: SCXK(J) 2014-0004). The animals were housed in controlled temperature ( $22\pm 1$  °C), relative humidity,  $55\pm 10\%$ , under a 12 h/12 h light-dark cycle with free get food and water. All the animal experiments were conducted according to the guidelines for animal care and use of China, and with the approval of ethical committee for animal experimentation at Lanzhou University. The mice were divided into three groups: control group (SAMR1 group), model group (SAMP8 group), and treatment group (SAMP8+ $\alpha$ -Linolenic acid, S30580, Shanghai Yuanye, China), the treatment group was administered with  $\alpha$ -Linolenic acid at 300 mg/kg by oral gavage, while the control group and model group were given an equivalent amount of normal saline respectively in the same fashion for 36 consecutive days.

### Brain tissue processing

All mice were quickly decapitated, the parietal bone was stripped along the coronal suture and sagittal suture to expose the brain tissue. The whole brain was taken out and fixed with 4% paraformaldehyde for Nissl's staining and Immunofluorescence; The cerebral cortex and hippocampus on one side of the mouse brain were dissected and froze in liquid nitrogen for RT-PCR and Western Blot; Tissue was removed, weighed, and put into a glass homogenizer filled with pre-cooled NS. The tissue was completely grinded on ice for 10 min and centrifuged at 4 °C, 3000 RPM for 10 min. The supernatant was retained in liquid nitrogen for ELISA.

### Morris water maze test

The Morris Water Maze (TM-Vision computer Behavior Experimental system WMT-00, Chengdu Thai Meng, China) test was used to detect spatial memory, and assess the working and reference memory functions in response to treatment. This behavioral test included visual platform trial (learning phase) which training mice to find a platform, hidden platform task and probe trail (test phase) which assessing whether mice had learned and remembered the location of the platform that was removed. First, the mice underwent 6 visual platform trials on the 30th day of intragastric administration. The different shapes and colors of waterproof paper was labeled on the bucket pool walls above the water in each quadrant so that the mice could orient itself to accomplish the goals. Next, the hidden platform task began on the 31st day of drug administration for 5 consecutive days. Before each experiment, each animal was placed on the platform to adapt for 15 s, and then separately released into the water from the S, W, and E quadrants toward the wall, allowing it to swim and find a visible platform in 60 s. If the animal finds the platform within 60 s, it was allowed to stay there for 15 s. If the mouse couldn't find the platform within 60 s, it was gently guided to the platform and allowed to stay there for 15 s. Each animal was tested 3 times a day,

with 5 minutes breaks between them. The times of reaching the platform and the effective area and escape incubation periods were collected for subsequent analysis. Finally, on the 36th day after administration, the probe trail was performed on mice with removing the platform from the pool. The percentage of time and moving distance spent in the target quadrant were recorded.

## ELISA analysis

The levels of Tau, acetylcholine (Ach) and glutamate (Glu) were measured using ELISA kits separately (Shanghai Yuanye, China). Before performance of the assays, the whole brain tissue homogenates were diluted 5 times. All samples were analyzed in duplicate according to the manufacturer's instructions. Optical density (OD) value at the wavelength of 450 nm was determined by a microplate reader (BS1101, Nanjing Detie, China), the concentration of these three factors in the sample was calculated according to the standard curve generated by continuous dilution of the standard substance in the kits.

## RT-PCR analysis

Total tissue RNA was extracted using TRIzol Reagent (Ambion, USA). The purity of RNA samples with A260/A280 values between 1.7 and 2.0 by Uv/nucleic acid protein detector (Modulus, Turner Biosystems, USA) were used for subsequent experiments. Firstly, 16  $\mu$ L of total RNA samples were reverse transcribed using Reverse transcription kit (Promega, USA) with the following protocol: 42 °C for 15 mins, 85 °C for 5 s, with a total of 4 cycles. Then, 2  $\mu$ L of cDNA was expanded using Amplification kit (Promega, USA) with the following protocol: the cDNA were denatured at 94 °C for 60 s, annealed at 60 °C for 1min, and extended at 68 °C for 2min, with a total of 40 cycles. All the Primers for TREK-1, GLT-1, NMDAR, GAPDH were designed using Primer Premier software (ver. 6.0, Premier Biosoft International, USA). Cycle threshold of samples and control housekeeping gene were analyzed according the  $2^{-\Delta\Delta Ct}$  expression, where  $\Delta Ct$  represents the relative gene levels of samples between the target gene and control gene GAPDH. The primer pairs were listed as follow: TREK-1 (118bp), forward: 5'-AAGGAAGAG GTGGGAGAGTT-3', Reverse: 5'-CACGCTGGAACCTTGT CATAGA-3'; GLT-1 (112bp), forward: 5'-ATGTCTTCGTGCATTCGGTGT TGGG-3', Reverse: 5'-AGCCGTGGCACCATGTTAATAGC-3'; NMDAR (104bp)), forward: 5'-AATGTGACGGCTCTGCTGATG-3', Reverse: 5'-TACCCAGAGC CCGTC ATGTT-3'; GAPDH (95bp), forward: 5'-AGGTCGGTGTGAACGGATTTG-3', Reverse: 5'-GGGGTCGTTGATGGCAACA-3' .

## Western blot analysis

Proteins from the cerebral cortex and hippocampus of mice were extracted using highly efficient RIPA tissue lysis buffer (Solarbio, China). The obtained protein concentrations were determined using a BCA protein quantification kit (Vazyme, nanjing, China). 10  $\mu$ L of protein samples were separated by 15% SDS-PAGE gels (SDS-PAGE gel electrophoresis kit, Solarbio, China), then electrophoretically transferred to a PVDF membrane. Afterwards, membranes were blocked in 5% skim milk on a thermostatic oscillator

(SHA-B, Jiangsu Youlian, China) for 1h at room temperature, followed by overnight incubation at 4 °C with the primary antibodies listed below: Rabbit anti mouse TREK-1 polyclonal antibody (1:1000, APC-047, alomone labs, Israel), Rabbit anti mouse GLT-1 polyclonal antibody (1:1500, G4005-9, US Biologicala, USA), Rabbit anti mouse NMDAR2B polyclonal antibody (1:1000, 4207, Cell Signaling Technology, USA) and Mouse anti-GAPDH mAb (1:1500, ZS-25778, Zhongshanjinqiao, China). After washing five times with TBST, the membranes were incubated with 1:5000 dilutions of Goat anti-rabbit polyclonal antibody (072-07-15-06, KPL, USA) on the thermostatic oscillator at room temperature for 1 hour then followed with six times of wash. Proteins were visualized using exposure machine (UniCel Dxl 800, Beckman Coulter, USA). The results were expressed as relative protein levels, that is, the expression level of each protein was monitored by the protein load of GAPDH.

## Immunofluorescence

The morphological changes of neurons and astrocytes were detected. Firstly, antigenic repair was performed on paraffin sections, the dehydrated paraffin sections were soaked in methanol containing 0.3% hydrogen peroxide for 10 mins, then in double distilled water 2 times, 2 mins each time. The sections were incubated with an antigen repair solution (PH6.0 citrate buffer) at 105 °C for 10 min, washed 3 times with PBS, and blocked with blocking buffer for 30 min at room temperature. After that, the slices incubated with Rabbit anti mouse Anti-GFAP monoclonal antibody (1:1000, ab207165, Abcam, UK) and Rabbit anti mouse Anti-NeuN monoclonal antibody (1:200, ab177487, Abcam, UK) overnight at 4 °C. After 3 times of wash, the slices were incubated with Goat anti-rabbit IgG (H+L) secondary antibody, FITC (1:100, A24532, Invitrogen, USA) in dark for 30 min, and then washed 3 times. The slides were co-incubated with DAPI staining solution in dark for 5 minutes, washed with PBS for 3 times, then sealed with anti-fluorescent quenching agent, and the edges of the cover glass were fixed with nail polish. Finally, image acquisition of slices was performed by fluorescence microscope (CX-23, OLYMPUS, Japan).

## Nissl staining

The paraffin sections were incubated at 60 °C for 5 h and dried. The slices were successively immersed in xylene for 10 min and another 5 min, then successively in 100%, 95%, 90%, 85% alcohol for 5 min. The slices were stained with Nissl staining kit (WX122-100, Beijing Huayueyang, China) according to the instructions at 56 °C for 1 h. Briefly the slices were soaked in distilled water for 8 min, and then differentiated in 95% alcohol for 1 min. then soaked with absolute alcohol for 2 times, xylene for 3 times, 2 min each time. Finally, slices were sealed with neutral gum, and the cortical areas were imaged under an optical microscope (DYS-102, Shanghai Zhaoyi, China).

## Statistical analysis

GraphPad Prism 8.0.2 (GraphPad Software, USA) statistical software was used for statistical analysis, and results were calculated as mean  $\pm$  standard error of the mean. Data were analyzed by one-way ANOVA for comparison between groups, and LSD was used for homogeneity of variance. Grade correlation analysis was conducted by Pearson correlation analysis between the detection index and monthly age, and the results were expressed by rank correlation coefficient.  $p < 0.05$  was statistically significant differences.

## Results

### **Tau, Ach and Glu levels in the brains of SAMP8 mice at different ages**

SAMP8 mice have been recognized as a model of age dependent neurodegenerative disease. To investigate the changes of Alzheimer's related proteins with the age, the levels of Tau, Ach and Glu in brains of SAMP8 mice at 1, 3, 6 and 9 months were measured. As shown in Fig. 1, a significant increase in levels of Tau and Glu and a significant decrease in levels of Ach were observed at age of 6, 9 months of SAMP8 mice when compared with 1 or 3-month-old SAMP8 mice ( $p < 0.01$  and  $p < 0.05$ ). Then the correlations between Tau, Ach, Glu levels and months were observed, as following that the levels of Tau and Glu in brains of SAMP8 mice increased gradually from 1 month to 9 months, and there was a positive grade correlation, the rank correlation coefficient was 0.893 ( $P = 0.000$ ) and 0.549 ( $P = 0.005$ ) respectively. Conversely, the level of Ach decreased over the month age, showed a negative correlation of grade with -0.912 of the rank correlation coefficient ( $P = 0.000$ ). This proved that with the increase of months, pathological accumulation of Tau proteins and Glu accompanied with the reduction of Ach were the pathological processes of SAMP8 mice, probably responsible for aggravation of the neurotoxicity and impaired the learning and cognitive abilities.

### **Levels of TREK-1 in SAMP8 mice at different ages**

To determine whether TREK-1 channel involved in the pathological process of Alzheimer's disease, the gene and protein expression levels of TREK-1 in brains of SAMP8 and SAMR1 mice aged 1, 3, 6 and 9 months were compared. As shown in Fig. 2, with the increase of month age, the levels of TREK-1 gene and protein in cerebral cortex and hippocampus of SAMR1 mice increased gradually. However, they showed an increasing trend at the age of 1 month and 3 months, and an opposite trend from 6 months to 9 months in SAMP8 mice. In addition, compared with age-matched SAMR1 mice, the expression levels of TREK-1 gene in cerebral cortex and hippocampus were significantly increased in SAMP8 mice aged 1 and 3 months ( $p < 0.01$ ), while decreased in SAMP8 mice aged 6 and 9 months ( $p < 0.05$ ). The results of TREK-1 protein levels were similar with that of gene, except that a dramatic drop occurred at 3 months ( $p < 0.05$ ). These results suggested that TREK-1 potassium channel is involved in the pathological process of SAMP8 mice. Because the levels of TREK-1 reduced significantly at 6 months, so 6-month-old SAMP8 mice were selected for further exploration.

# Effects of ALA treatment on learning and memory of SAMP8 mice

Much documents have been proved that TREK-1 potassium channel is activated by polyunsaturated fatty acids (Lauritzen et al. 2000). Next,  $\alpha$ -Linolenic acid (ALA) was used as an activator of TREK-1 channel to evaluate the effects of TREK-1 on learning and memory functions in aged SAMP8 mice by Morris water maze test.

## Effects of ALA on hidden platform task

The times of reaching the platform and entering effective area was greatly reduced in SAMP8 compared to SAMR1 ( $p < 0.01$ ). SAMP8 treated with 300 mg/kg ALA for 36 days showed significantly decreased times of reaching the platform and entering effective area compared with that of untreated SAMP8 ( $p < 0.05$ ).

The escape latency helps to determine the time spent that mice reached the platform. As shown in Fig. 3, results of the group comparisons suggested that the escape latency of SAMP8 was significant longer than that of SAMR1 and SAMP8 treated with ALA ( $p < 0.01$ ). ALA treatment significantly improved the spatial memory retention as indicated by marked reduction of latency compared with SAMP8 mice ( $p < 0.05$ ). These results indicated that SAMP8 mice showed the significant learning deficits, and ALA improved the spatial learning abilities in SAMP8.

## Effects of ALA on probe trail

The results from the probe trial showed a putative measurement of spatial memory retention. As shown in Fig. 3, SAMP8 mice spent significant less times in entering platform area and effective area than that of SAMR1, whereas treatment with ALA increased entering times of SAMP8 ( $p < 0.01$ ). The percent time and distance spent in target quadrant by SAMP8 mice were significantly lower than those of SAMR1 mice ( $p < 0.01$ ), SAMP8 mice with ALA treatment showed a marked improvement in their ethological performance as their percent time and distance spent in target quadrant were significantly prolonged ( $p < 0.05$ ).

The swimming trajectory of mice was shown in Fig. 3. After the platform was removed, the SAMR1 mice had a very accurate memory on the position of the platform, and had been shuttling around the platform; However, the swimming track of SAMP8 mice was not related to the platform position. In contrast, SAMP8 mice in the ALA intervention group significantly increased the number of shuttles in the effective platform area. These results indicated that SAMP8 mice showed significant memory deficits, and ALA improved the spatial memory retention in SAMP8.

# Morphological changes

The morphology of neurons, astrocytes and Nissl bodies in the cerebral cortex, hippocampus of mice was observed by immunofluorescence and Nissl staining. As shown in Fig. 4, 5, in the cerebral cortex and hippocampus of SAMR1 mice, the neurons were large and intact, astrocytes were evenly arranged among neurons, it had very high fluorescence intensity. In SAMP8 mice, the number of surviving neurons and astrocytes were significantly reduced, most of them were edema and loosely arranged. The percentage of NeuN (+) cells and GFAP (+) cells decreased significantly ( $p < 0.01$ ) and the fluorescence intensity was weak, suggested that the neurons and astrocytes in SAMP8 mice had apoptosis, loss part of the function. In the SAMP8 mice after ALA treatment, lots of neurons and astrocytes with complete structure were found in cerebral cortex and hippocampus. Compared with SAMP8 mice, the percentages of NeuN (+) cells and GFAP (+) cells increased significantly ( $p < 0.01$ ), but the fluorescence intensity is abated. Those showed that some of the neurons and astrocytes were damaged during the pathological changes of SAMP8 mice, ALA rescued the apoptotic cells.

As shown in Fig. 6, Nissl bodies in cerebral cortex and hippocampus of SAMR1 mice were abundant and evenly distributed. However, the number of Nissl bodies in cerebral cortex and hippocampus of SAMP8 mice were significantly reduced in comparison to SAMR1 mice ( $p < 0.01$ ), most of these Nissl bodies were disintegrated, accompanied by a tendency of gradually expanding outwards until dissolution and disappearance, indicating the loss of neuronal function and serious impairment of brain function. Meanwhile, the number of Nissl bodies in cerebral cortex and hippocampus in SAMP8 mice treated with ALA were significantly improved compared with those of SAMP8 mice ( $p < 0.01$ ), and they were intact and well-defined. The results suggested the activation of TREK-1 potassium channel may improve the function of impaired neurons in SMP8 mice.

## Levels of TREK-1 in SAMP8 mice treated with ALA

As shown in Fig. 7, the gene and protein levels of TREK-1 in cerebral cortex and hippocampus of SAMP8 mice were significantly decreased ( $p < 0.01$ ) compared with those of SAMR1 mice. ALA treatment significantly increased the expression levels of TREK-1 gene and protein both in cerebral cortex and hippocampus of SAMP8 mice ( $p < 0.05$ ). Intervention of ALA in SAMP8 mice showed the activation of TREK-1 potassium channel might help to improve the learning and memory deficits.

## Effects of ALA on Glutamate metabolic pathway in SAMP8 mice

TREK-1 channel has been found to have neuroprotective effects in many brain diseases. It mediated the release of Glu by astrocytes to regulate the synaptic connection between astrocytes and neuron (Lalo et al. 2014 ; Woo et al. 2012). AA *exert* protective effect on oxygen-glucose deprived astrocytes by

increasing glutamate reuptake(Lu et al. 2017). The accumulation of Glu leads to over-activation of NMDAR, resulting in neuronal damage(Ota et al. 2015). In order to determine the effect of TREK-1 channel on the glutamate metabolism pathway, the levels of Glu, GLT-1 and NMDAR were observed by ELISA and RT-PCR and Western Blot. As shown in Fig. 7, SAMP8 mice showed significantly higher levels of Glu ( $p<0.01$ ) and NMDAR ( $p<0.01$ ) and lower levels of GLT-1 ( $p<0.01$ ) in the brain compared with SAMR1 mice. The results suggested that SAMP8, might reduce GLT-1-related Glu uptake, leading to a large accumulation of Glu in the brain, increasing the binding of Glu to its receptor NMDAR, and thus aggravate the Glu-mediated neurotoxicity in the process of AD. Reversely, the level of Glu ( $p<0.01$ ) and the gene and protein expression levels of NMDAR ( $p<0.05$ ) in SAMP8 treated with ALA were significantly reduced, and those of GLT-1 ( $p<0.05$ ) were significantly improved compared with SAMP8 mice. ALA, as an activator of TREK-1 channel, accelerated the transport of Glu by up-regulating the level of GLT-1, reducing the accumulation of Glu and the binding of Glu to NMDAR, in the brain, effectively alleviating the neurotoxicity. Results proved that the activation of TREK-1 channel improves learning and memory function in SAMP8 mice through a glutamate metabolism pathway.

## Discussion

Researches have demonstrated that the two pore potassium channel TREK-1 plays the protective role in central nervous disorders(Djillani et al. 2019). However, to our best knowledge, no findings concerned about the role of TREK-1 in AD. In the present study, we investigated the change trend of TREK-1 channel in brains of SAMP8 mice and showed the expression levels of TREK-1 compensatory arose before 3 months of age, then began to decline. Next, we showed activation of TREK-1 channel by ALA improved the learning and memory deficits of SAMP8 mice aged in 6 months. Furthermore, we explored the possible mechanisms and found that the levels of active molecules were closely related to the glutamate metabolism pathway. After the activation of TREK-1 channel, the damaged neurons and astrocyte were rescued, the levels of Glu and NMDAR were down-regulated, while the level of GLT-1 was significantly increased.

As we known, Tau is a microtubule-associated protein that aggregates to form Neurofibrillary tangles (NFTs) (Gao et al. 2018). Pathological deposition of abnormal Tau in the brain and/or the loss of its function may an important cause of AD (Miyasaka et al. 2018). Although studies have shown that elevated Tau levels are the biomarker for AD (Tsolaki et al. 2001), the tendency of Tau levels during the pathological process of AD is seldom reported. Our results showed that with the increase of the month age of SAMP8 mice, the Tau content in their brains increased hierarchically, suggesting the amount of accumulated Tau is positive proportional to the severity of AD. Similar to Tau, Ach also reflects the impairment of learning and memory function to a certain extent (Min et al. 2010). Enhancement of cholinergic activity mediates the improvement of cognitive function (Smith et al. 2002). Studies have confirmed that in the brain of AD model mice, the increase of Glu leads to the apoptosis of hippocampal neurons and inhibition of Glu content reduce the brain injury (Fuhrmann et al. 2010). Consistent with this, our results showed the Glu content increased hierarchically, while the Ach decreased hierarchically from 1 month to 9 months aged of SAMP8 mice. In general, gradually increased Tau and Glu and decreased Ach

were associated with the pathological a process of SAMP8 mice, and the older the mice were, the worse the condition was. Although some pathological changes could be reversed, the early application of drugs such as AchE inhibitors and Glu receptor antagonists can reduce the damage of nerve cells and effectively improve the learning and memory function.

To decipher whether TREK-1 potassium channel involved in the pathological process of AD, the protein and gene levels of TREK-1 were compared in different months of SAMP8 and SAMR1 mice. The results indicated the gene and protein levels of TREK-1 in the cerebral cortex and hippocampus gradually increased with the age in SAMR1 mice. However, the expression of TREK-1 was at a higher level in SAMP8 mice at 1 to 3 months of age, and decreased significantly at 6 and 9 months of age. This change suggested that the TREK-1 might be a protector factors participating in the process of AD. SAMP8 mice in the early of life show the symptoms of aging, accelerated the TREK-1 channel expression level to obtain their own adjustment. But with the development of AD, a series of pathological changes, such as the damaged structure of nerve cells, apoptosis of synapses, beyond the scope of the body itself can be adjusted. This may be responsible for the reduced TREK-1 expression in older SAMP8 mice. PUFAs are the recognized potent activator of TREK-1 and exert the beneficial effects in the prevention of central nervous disease. Here, ALA was used as an agonist of TREK-1. The TREK-1 channel is heavily activated from the low-expression state as the decreased TREK-1 levels were significantly up-regulated after ALA intervention. Next, we further verified the activation effect of TREK-1 on AD from the aspects of behavior, cell morphology, and the mechanism of action.

Learning and memory disorders are the most prominent symptoms of AD, so Morris water maze test was used to detect the spatial learning and memory ability of SAMP8 mice after ALA intervention. These results reflected that after activation of the TREK-1 channel, SAMP8 mice significantly increased their ability to search platform and maintain spatial memory after continuous training. ALA facilitated the reconstruction of the injured structure of Nissl bodies, neurons, and astrocytes probably were the material basis for improving the learning and memory ability of SAMP8 mice.

Glu is involved in many processes in the brain, including cognition, movement and development (Hascup et al. 2008). Paradoxically, overloaded Glu mediates excessive activation of neurotoxic effect (Sun et al. 2018). The dynamic balance of Glu content is maintained by glutamate transport system on membrane of astrocytes (Mahmoud et al. 2019). Five subtypes of glutamate transporters have been isolated, and GLT-1 subtypes, which are widely distributed in the central nervous system, have been selected. NMDAR is the main receptor for Glu mediated neurotoxic injury and is most densely distributed in the cerebral cortex and hippocampus. Under pathological conditions, GLT-1 reduces the uptake of Glu, and even reverses the transport to the extracellular, aggravating the cytotoxic effect of Glu (Yi et al. 2005). Excessive excitation of NMDAR by a large amount of Glu leads to a large amount of  $Ca^{2+}$  influx and the formation of intracellular  $Ca^{2+}$  overload, which is an important way to cause cell dysfunction and induce cell apoptosis (Gu et al. 2009). Studies have confirmed that GLT-1 expression and glutamate uptake capacity were decreased, accelerating cognitive deficit in AD animal models (Meeker et al. 2015 ; Mookherjee et al. 2011). Consistent with this, we also showed the similar changes with increased Glu content and

decreased level of GLT-1 which indicated the formation of neurodegenerative changes in SAMP8 mice. TREK-1 has been confirmed to take part in regulation of GLT-1 activity (Lu et al. 2017). In cerebral ischemia, TREK-1 regulated GLT-1 activity and improved synaptic connections (Lalo et al. 2014). Activated TREK-1 channels inhibited NMDAR and improved the function of blood-brain barrier (Bittner et al. 2013) and improved cerebral ischemia by rescuing the protein abundance of GLT-1 (Liu et al. 2014). In this study, Glu and NMDAR expression levels in the cerebral cortex and hippocampus of SAMP8 mice after activation of TREK-1 potassium channels were decreased significantly, while GLT-1 expression level were increased significantly that explained treatment of ALA effectively improved the neurotoxic effect caused by Glu accumulation, also showed glutamate metabolic pathways involved in the improvement of cognitive deficits. Our results intuitively reflect the close relationship between the potassium channels of TREK-1 and glutamate metabolism pathway in the pathological process of AD. Therefore, the regulation of glutamate metabolism pathway through TREK-1 potassium channel is likely to be a new pathway for the treatment of AD.

In conclusions, the present study demonstrated that TREK-1 participated in the pathological process of AD in SAMP8 mice. Activation of the TREK-1 potassium channel improved learning and memory deficits and underlying mechanisms is related to modulation of glutamate metabolic pathway. The TREK-1 potassium channel may be expected to be a new potential therapeutic target for AD.

## Declarations

**Funding** This study was supported by foundation of key laboratory of Chinese medicine innovation and transformation in Gansu Province/Chinese medicine product engineering laboratory of Gansu Province (ZYFYZH-KJ-2016-004) and Talent Innovation and Entrepreneurship Science and Technology projects of Lanzhou city (2015-RC-20)

**Conflict of interest** All authors declare that they are no conflicts of interest regarding the publication of this article.

**Data availability** Data supporting the results of this study are available upon reasonable request of the corresponding author.

**Code availability** NOT applicable.

Author contributions F Li has full access to all data in the study and is responsibility for the integrity of the data and the accuracy of the data analysis. SN Zhou and F Li contributed equally to this work and are co-first authors. F Li collected the data, drafted and revised the manuscript. SN Zhou analyzed the data. X Zeng did animal experiments, R Yang and XX Wang contributed to section staining. B Meng and WL Pei collected the data. L Li designed the study, F Li interpreted data and reviewed the manuscript. L Li and XX Wang did critical revision of the manuscript. All authors read and approved the final manuscript.

**Ethical approval** All the animal experiments were conducted according to the guidelines for animal care and use of China. The authors also confirm that the study was performed in accordance with the approval of ethical committee for animal experimentation at Lanzhou University.

**Consent to participate** NOT applicable.

**Consent for publication** NOT applicable.

## Acknowledgments

We thank the members of the Lu li Laboratory, Institute of Pharmacology, Lanzhou University School of Basic Medicine, for their constructive feedback on the production of this manuscript. We also thank the Key Laboratory of Traditional Chinese Medicine Innovation and Transformation of Gansu Province/Engineering Laboratory of Traditional Chinese Medicine Products of Gansu Province (ZYFYZH-KJ-2016-004) and the Talent Innovation and Entrepreneurial Science and Technology Project of Lanzhou City (2015-RC-20) for providing funding for this study.

## References

- Akiguchi I, Pallàs M, Budka H, Akiyama H, Ueno M, Han J et al (2017) SAMP8 mice as a neuropathological model of accelerated brain aging and dementia: Toshio Takeda's legacy and future directions. *Neuropathology* 37(4):293-305. <https://doi.org/10.1111/neup.12373>
- Bittner S, Ruck T, Schuhmann MK, Herrmann AM, Moha ou Maati H, Bobak N et al (2013) Endothelial TWIK-related potassium channel-1 (TREK1) regulates immune-cell trafficking into the CNS. *Nat Med* 19(9):1161-1165. <https://doi.org/10.1038/nm.3303>
- Blokland A, Honig WR, Raaijmakers WG (1992) Effects of intra-hippocampal scopolamine injections in a repeated spatial acquisition task in the rat. *Psychopharmacology (Berl)* 109(3):373-376. <https://doi.org/10.1007/bf02245886>
- Boccia MM, Acosta GB, Blake MG, Baratti CM (2004) Memory consolidation and reconsolidation of an inhibitory avoidance response in mice: effects of i.c.v. injections of hemicholinium-3. *Neuroscience* 124(4):735-741. <https://doi.org/10.1016/j.neuroscience.2004.01.001>
- Boccia MM, Blake MG, Acosta GB, Baratti CM (2003) Atropine, an anticholinergic drug, impairs memory retrieval of a high consolidated avoidance response in mice. *Neurosci Lett* 345(2):97-100. [https://doi.org/10.1016/s0304-3940\(03\)00493-2](https://doi.org/10.1016/s0304-3940(03)00493-2)
- Boccia MM, Blake MG, Baratti CM, McGaugh JL (2009) Involvement of the basolateral amygdala in muscarinic cholinergic modulation of extinction memory consolidation. *Neurobiol Learn Mem* 91(1):93-97. <https://doi.org/10.1016/j.nlm.2008.07.012>

Chapman CG, Meadows HJ, Godden RJ, Campbell DA, Duckworth M, Kelsell RE et al (2000) Cloning, localisation and functional expression of a novel human, cerebellum specific, two pore domain potassium channel. *Brain Res Mol Brain Res* 82(1-2):74-83. [https://doi.org/10.1016/s0169-328x\(00\)00183-2](https://doi.org/10.1016/s0169-328x(00)00183-2)

Danysz W, Wroblewski J, Costa E (1988) Learning impairment in rats by N-methyl-D-aspartate receptor antagonists. *Neuropharmacology* 27(6):653-656. [https://doi.org/10.1016/0028-3908\(88\)90189-x](https://doi.org/10.1016/0028-3908(88)90189-x)

Djillani A, Mazella J, Heurteaux C, Borsotto M (2019) Role of TREK-1 in Health and Disease, Focus on the Central Nervous System. *Front Pharmacol* 10:379. <https://doi.org/10.3389/fphar.2019.00379>

Ferraguti F, Crepaldi L, Nicoletti F (2008) Metabotropic glutamate 1 receptor: current concepts and perspectives. *Pharmacol Rev* 60(4):536-581. <https://doi.org/10.1124/pr.108.000166>

Ferreira-Vieira TH, Guimaraes IM, Silva FR, Ribeiro FM (2016) Alzheimer's disease: Targeting the Cholinergic System. *Curr Neuropharmacol* 14(1):101-115. <https://doi.org/10.2174/1570159x13666150716165726>

Fuhrmann M, Bittner T, Jung CK, Burgold S, Page RM, Mitteregger G et al (2010) Microglial Cx3cr1 knockout prevents neuron loss in a mouse model of Alzheimer's disease. *Nat Neurosci* 13(4):411-413. <https://doi.org/10.1038/nn.2511>

Gao Y, Tan L, Yu J, Tan L (2018) Tau in Alzheimer's Disease: Mechanisms and Therapeutic Strategies. *Curr Alzheimer Res* 15(3):283-300. <https://doi.org/10.2174/1567205014666170417111859>

Goedert M, Spillantini MG (2006) A century of Alzheimer's disease. *Science* 314(5800):777-781. <https://doi.org/10.1126/science.1132814>

Gu B, Nakamichi N, Zhang WS, Nakamura Y, Kambe Y, Fukumori R et al (2009) Possible protection by notoginsenoside R1 against glutamate neurotoxicity mediated by N-methyl-D-aspartate receptors composed of an NR1/NR2B subunit assembly. *J Neurosci Res* 87(9):2145-2156. <https://doi.org/10.1002/jnr.22021>

Hascup KN, Hascup ER, Pomerleau F, Huettl P, Gerhardt GA (2008) Second-by-second measures of L-glutamate in the prefrontal cortex and striatum of freely moving mice. *J Pharmacol Exp Ther* 324(2):725-731. <https://doi.org/10.1124/jpet.107.131698>

Hervieu GJ, Cluderay JE, Gray CW, Green PJ, Ranson JL, Randall AD et al (2001) Distribution and expression of TREK-1, a two-pore-domain potassium channel, in the adult rat CNS. *Neuroscience* 103(4):899-919. [https://doi.org/10.1016/s0306-4522\(01\)00030-6](https://doi.org/10.1016/s0306-4522(01)00030-6)

Heurteaux C, Guy N, Laigle C, Blondeau N, Duprat F, Mazzuca M et al (2004) TREK-1, a K<sup>+</sup> channel involved in neuroprotection and general anesthesia. *EMBO J* 23(13):2684-2695. <https://doi.org/10.1038/sj.emboj.7600234>

- Honoré E (2007) The neuronal background K2P channels: focus on TREK1. *Nat Rev Neurosci* 8(4):251-261. <https://doi.org/10.1038/nrn2117>
- Jeong S (2017) Molecular and Cellular Basis of Neurodegeneration in Alzheimer's Disease. *Mol Cells* 40(9):613-620. <https://doi.org/10.14348/molcells.2017.0096>
- Knox D (2016) The role of basal forebrain cholinergic neurons in fear and extinction memory. *Neurobiol Learn Mem* 133:39-52. <https://doi.org/10.1016/j.nlm.2016.06.001>
- Lalo U Palygin O Rasooli-Nejad S Andrew J Haydon P Pankratov Y (2014) Exocytosis of ATP from astrocytes modulates phasic and tonic inhibition in the neocortex. *PLoS Biol* 12(1):e1001747. <https://doi.org/10.1371/journal.pbio.1001747>
- Lauritzen I Blondeau N Heurteaux C Widmann C Romey G Lazdunski M (2000) Polyunsaturated fatty acids are potent neuroprotectors. *EMBO J* 19(8):1784-1793. <https://doi.org/10.1093/emboj/19.8.1784>
- Liu Y Sun Q Chen X Jing L Wang W Yu Z et al (2014) Linolenic acid provides multi-cellular protective effects after photothrombotic cerebral ischemia in rats. *Neurochem Res* 39(9):1797-1808. <https://doi.org/10.1007/s11064-014-1390-3>
- Lu L Zhang G Song C Wang X Qian W Wang Z et al (2017) Arachidonic acid has protective effects on oxygen-glucose deprived astrocytes mediated through enhancement of potassium channel TREK-1 activity. *Neurosci Lett* 636:241-247. <https://doi.org/10.1016/j.neulet.2016.11.034>
- Mahmoud S Gharagozloo M Simard C Gris D (2019) Astrocytes Maintain Glutamate Homeostasis in the CNS by Controlling the Balance between Glutamate Uptake and Release. *Cells* 8(2). <https://doi.org/10.3390/cells8020184>
- Meeker KD Meabon JS Cook DG (2015) Partial Loss of the Glutamate Transporter GLT-1 Alters Brain Akt and Insulin Signaling in a Mouse Model of Alzheimer's Disease. *J Alzheimers Dis* 45(2):509-520. <https://doi.org/10.3233/jad-142304>
- Min SW Cho SH Zhou Y Schroeder S Haroutunian V Seeley WW et al (2010) Acetylation of tau inhibits its degradation and contributes to tauopathy. *Neuron* 67(6):953-966. <https://doi.org/10.1016/j.neuron.2010.08.044>
- Miyasaka T Shinzaki Y Yoshimura S Yoshina S Kage-Nakadai E Mitani S et al (2018) Imbalanced Expression of Tau and Tubulin Induces Neuronal Dysfunction in *C. elegans* Models of Tauopathy. *Front Neurosci* 12:415. <https://doi.org/10.3389/fnins.2018.00415>
- Mookherjee P Green PS Watson GS Marques MA Tanaka K Meeker KD et al (2011) GLT-1 loss accelerates cognitive deficit onset in an Alzheimer's disease animal model. *J Alzheimers Dis* 26(3):447-455. <https://doi.org/10.3233/jad-2011-110503>

Morris RG (1989) Synaptic plasticity and learning: selective impairment of learning rats and blockade of long-term potentiation in vivo by the N-methyl-D-aspartate receptor antagonist AP5. *J Neurosci* 9(9):3040-3057. <https://doi.org/10.1523/jneurosci.09-09-03040.1989>

Nakanishi SMasu M (1994) Molecular diversity and functions of glutamate receptors. *Annu Rev Biophys Biomol Struct* 23:319-348. <https://doi.org/10.1146/annurev.bb.23.060194.001535>

Ota H Oogawa S Ouchi Y Akishita M (2015) Protective effects of NMDA receptor antagonist, memantine, against senescence of PC12 cells: A possible role of nNOS and combined effects with donepezil. *Exp Gerontol* 72:109-116. <https://doi.org/10.1016/j.exger.2015.09.016>

Power AE Vazdarjanova A McGaugh JL (2003) Muscarinic cholinergic influences in memory consolidation. *Neurobiol Learn Mem* 80(3):178-193. [https://doi.org/10.1016/s1074-7427\(03\)00086-8](https://doi.org/10.1016/s1074-7427(03)00086-8)

Revett TJ Baker GB Jhamandas J Kar S (2013) Glutamate system, amyloid  $\beta$  peptides and tau protein: functional interrelationships and relevance to Alzheimer disease pathology. *J Psychiatry Neurosci* 38(1):6-23. <https://doi.org/10.1503/jpn.110190>

Riederer P Hoyer S (2006) From benefit to damage. Glutamate and advanced glycation end products in Alzheimer brain. *J Neural Transm (Vienna)* 113(11):1671-1677. <https://doi.org/10.1007/s00702-006-0591-6>

Shankar GM Bloodgood BL Townsend M Walsh DM Selkoe DJ Sabatini BL (2007) Natural oligomers of the Alzheimer amyloid-beta protein induce reversible synapse loss by modulating an NMDA-type glutamate receptor-dependent signaling pathway. *J Neurosci* 27(11):2866-2875. <https://doi.org/10.1523/jneurosci.4970-06.2007>

Smith JW Evans AT Costall BS Smythe JW (2002) Thyroid hormones, brain function and cognition: a brief review. *Neurosci Biobehav Rev* 26(1):45-60. [https://doi.org/10.1016/s0149-7634\(01\)00037-9](https://doi.org/10.1016/s0149-7634(01)00037-9)

Sofroniew MV Vinters HV (2010) Astrocytes: biology and pathology. *Acta Neuropathol* 119(1):7-35. <https://doi.org/10.1007/s00401-009-0619-8>

Sun Y Yang J Hu X Gao X Li Y Yu M et al (2018) Conditioned medium from overly excitatory primary astrocytes induced by La(3+) increases apoptosis in primary neurons via upregulating the expression of NMDA receptors. *Metallomics* 10(7):1016-1028. <https://doi.org/10.1039/c8mt00056e>

Tom SE Hubbard RA Crane PK Haneuse SJ Bowen J McCormick WC et al (2015) Characterization of dementia and Alzheimer's disease in an older population: updated incidence and life expectancy with and without dementia. *Am J Public Health* 105(2):408-413. <https://doi.org/10.2105/ajph.2014.301935>

Tsolaki M Sakka V Gerasimou G Dimacopoulos N Chatzizisi O Fountoulakis KN et al (2001) Correlation of rCBF (SPECT), CSF tau, and cognitive function in patients with dementia of the Alzheimer's type, other

types of dementia, and control subjects. *Am J Alzheimers Dis Other Demen* 16(1):21-31.  
<https://doi.org/10.1177/153331750101600107>

Vivier D, Bennis K, Lesage F, Ducki S (2016) Perspectives on the Two-Pore Domain Potassium Channel TREK-1 (TWIK-Related K(+) Channel 1). A Novel Therapeutic Target? *J Med Chem* 59(11):5149-5157.  
<https://doi.org/10.1021/acs.jmedchem.5b00671>

Wang W, Liu D, Xiao Q, Cai J, Feng N, Xu S et al (2018) Lig4-4 selectively inhibits TREK-1 and plays potent neuroprotective roles in vitro and in rat MCAO model. *Neurosci Lett* 671:93-98.  
<https://doi.org/10.1016/j.neulet.2018.02.015>

Winters BD, Bussey TJ (2005) Removal of cholinergic input to perirhinal cortex disrupts object recognition but not spatial working memory in the rat. *Eur J Neurosci* 21(8):2263-2270.  
<https://doi.org/10.1111/j.1460-9568.2005.04055.x>

Woo DH, Han KS, Shim JW, Yoon BE, Kim E, Bae JY et al (2012) TREK-1 and Best1 channels mediate fast and slow glutamate release in astrocytes upon GPCR activation. *Cell* 151(1):25-40.  
<https://doi.org/10.1016/j.cell.2012.09.005>

Yarishkin O, Phuong TTT, Bretz CA, Olsen KW, Baumann JM, Lakk M et al (2018) TREK-1 channels regulate pressure sensitivity and calcium signaling in trabecular meshwork cells. *J Gen Physiol* 150(12):1660-1675. <https://doi.org/10.1085/jgp.201812179>

Yi JH, Pow DV, Hazell AS (2005) Early loss of the glutamate transporter splice-variant GLT-1v in rat cerebral cortex following lateral fluid-percussion injury. *Glia* 49(1):121-133.  
<https://doi.org/10.1002/glia.20099>

## Figures

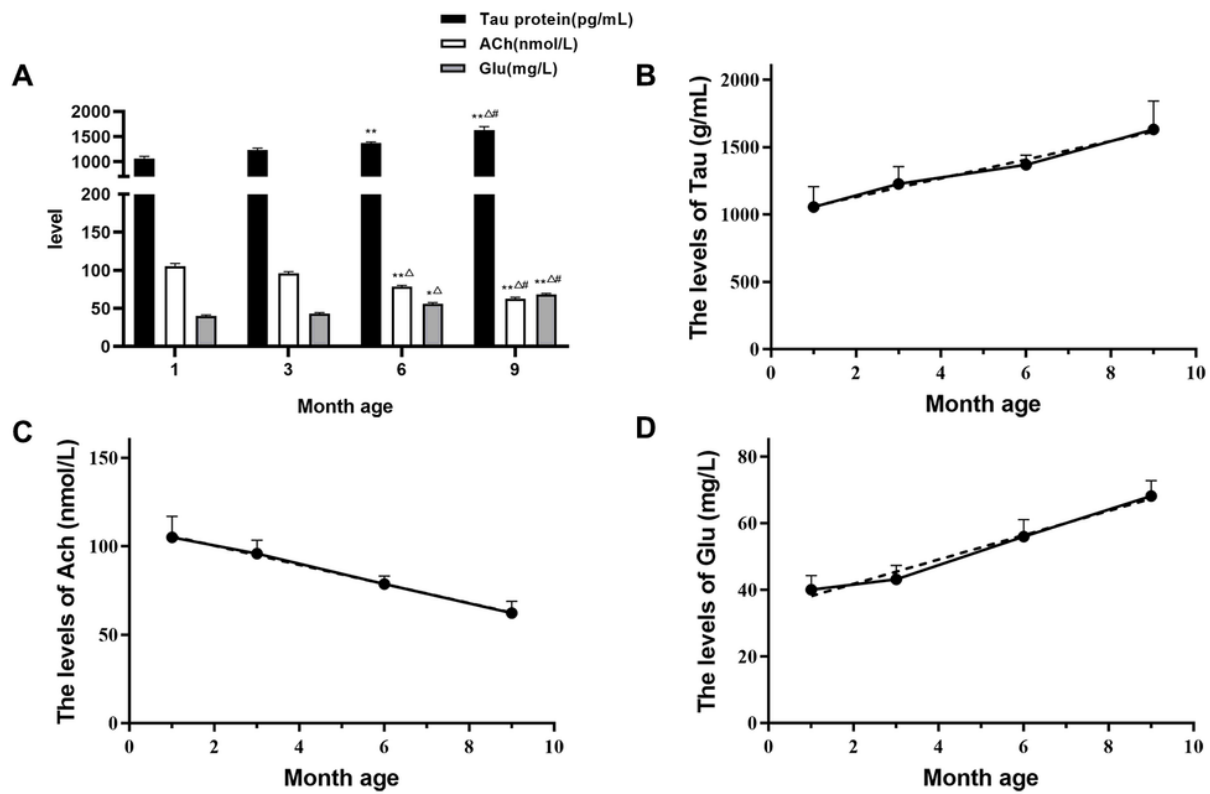


**Figure 1**

Tau, Ach and Glu levels in brains of SAMP8 mice at different ages (n=10). (a) The levels of Tau, Ach and Glu in brains of 1-, 3-, 6-, 9-month-old SAMP8 mice were compared, respectively (n=10). With the aging of SAMP8 mice, the trends of Tau (b) and Glu (d) levels were increased, while the Ach (c) was decreased. Data are presented as the mean±SEM. \*P<0.05, \*\*P<0.01 vs. 1-month-old SAMP8 mice; ΔP<0.05, ΔΔP<0.01 vs. 3-month-old SAMP8 mice; #P<0.05, ##P<0.01 vs. 6-month-old SAMP8 mice.

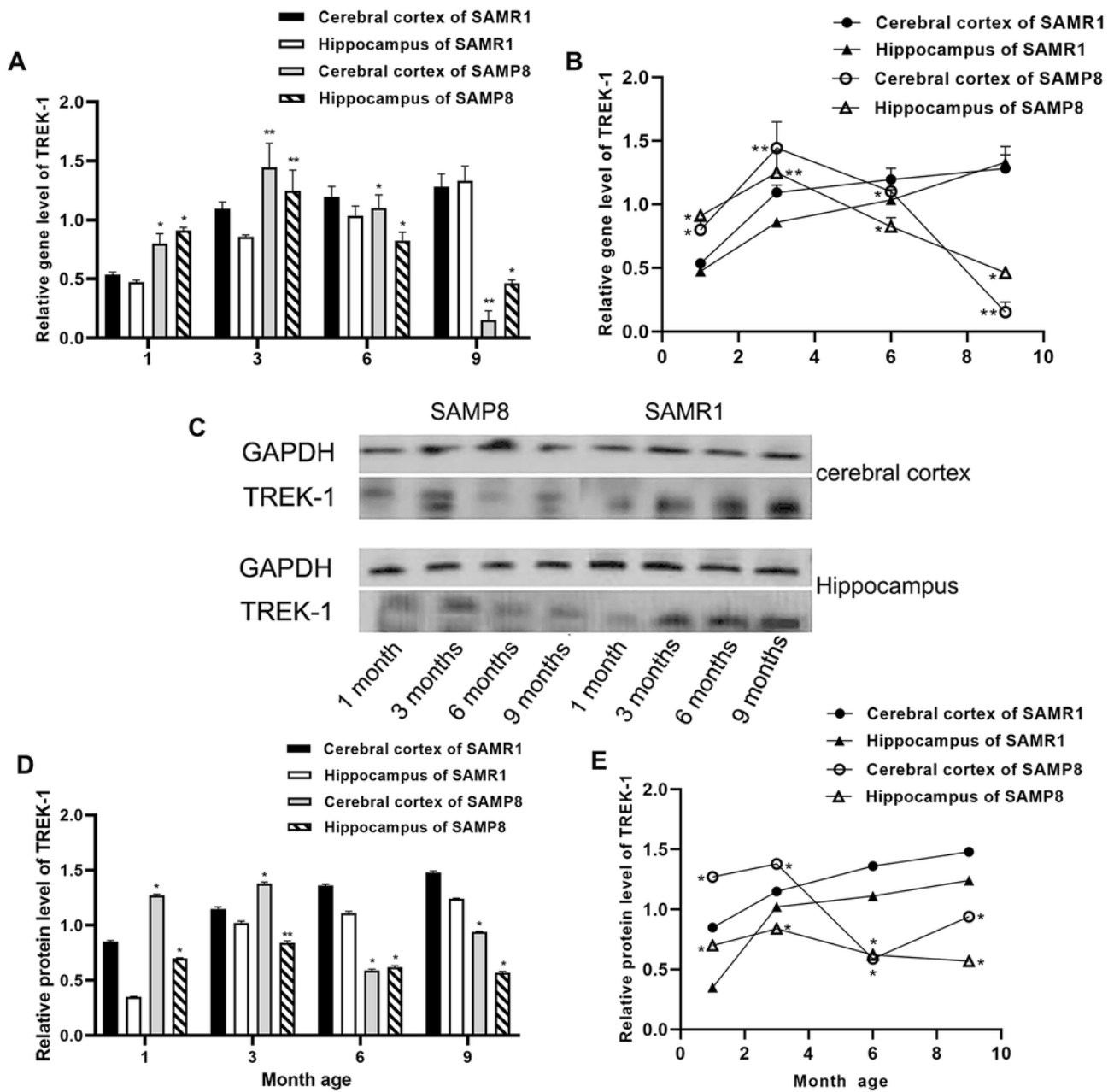


**Figure 2**

Gene and protein levels of TREK-1 in SAMR1 and SAMP8 mice at different ages (a) The TREK-1 gene levels in the cortex and hippocampus of SAMR1 mice at different age were compared with SAMP8 mice at the same age (n=5), and their variation trend with the increase of month age (b). (c) The expression bands of TREK-1 protein in the cortex and hippocampus of SAMP8 and SAMR1 mice at different age (n=3). (d) The TREK-1 protein levels in the cortex and hippocampus of SAMP8 were compared with SAMR1 mice at the same age, and their variation trend with the growth of the month age (e). Data are presented as the mean±SEM. \*p<0.05, \*\*p<0.01 vs age-matched SAMR1 mice.

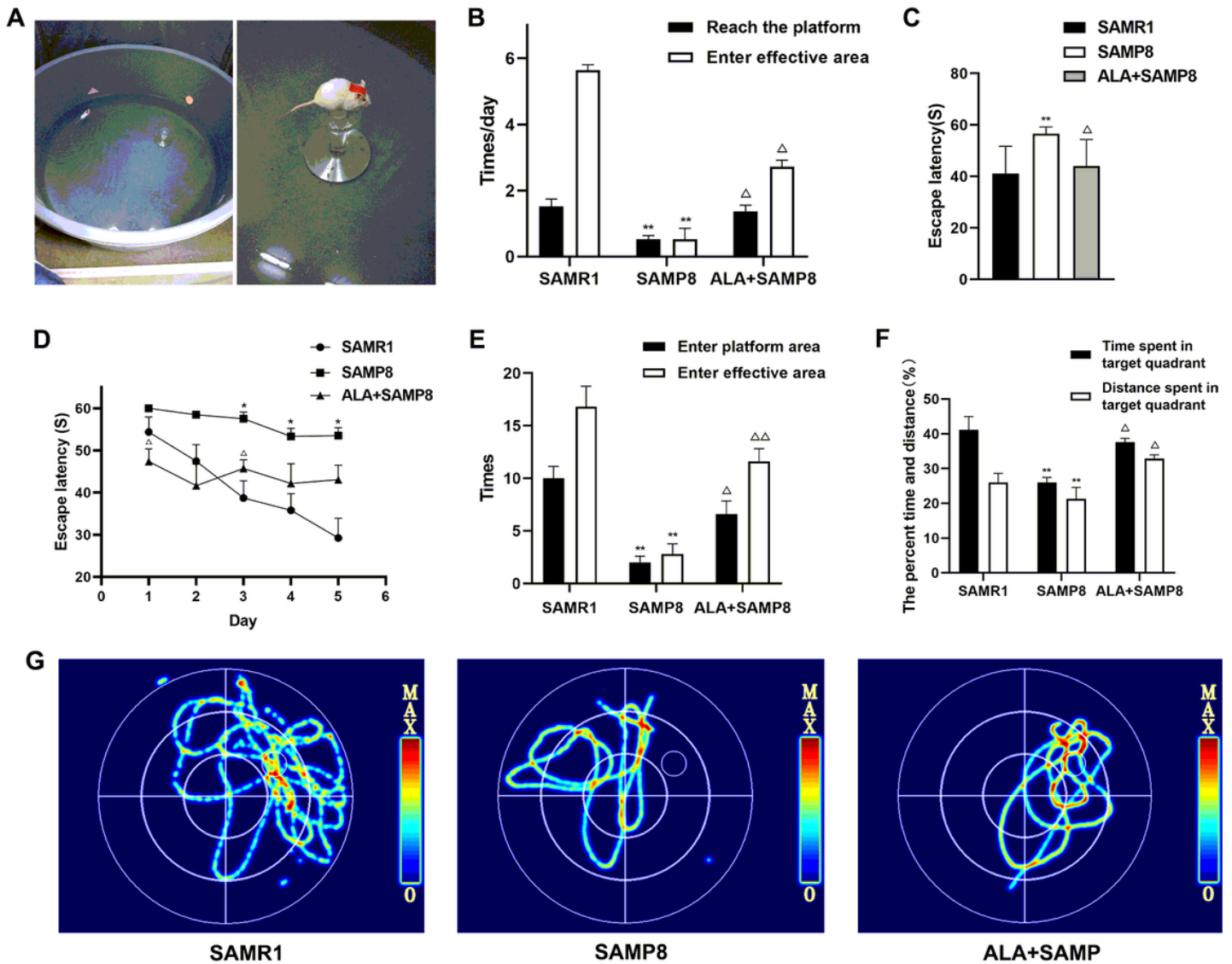


**Figure 3**

Results of Morris Water Maze Test (n=10) (a) Pictures taken during the water maze experiments. Hidden platform task: (b) The number of times for mice to reach the platform and effective area; Comparison (c) and trend (d) of escape latency of mice within 5 days. Probe trail: (e) The number of times for mice to enter the platform area and effective area; (f) The percent time and distance spent in target quadrant of mice were compared; (g) The data of swimming trajectory of mice. Data are presented as the mean $\pm$ SEM. \*P<0.05, \*\*P<0.01 vs. SAMR1 mice;  $\Delta$ P<0.05,  $\Delta\Delta$ P<0.01 vs. SAMP8 mice.

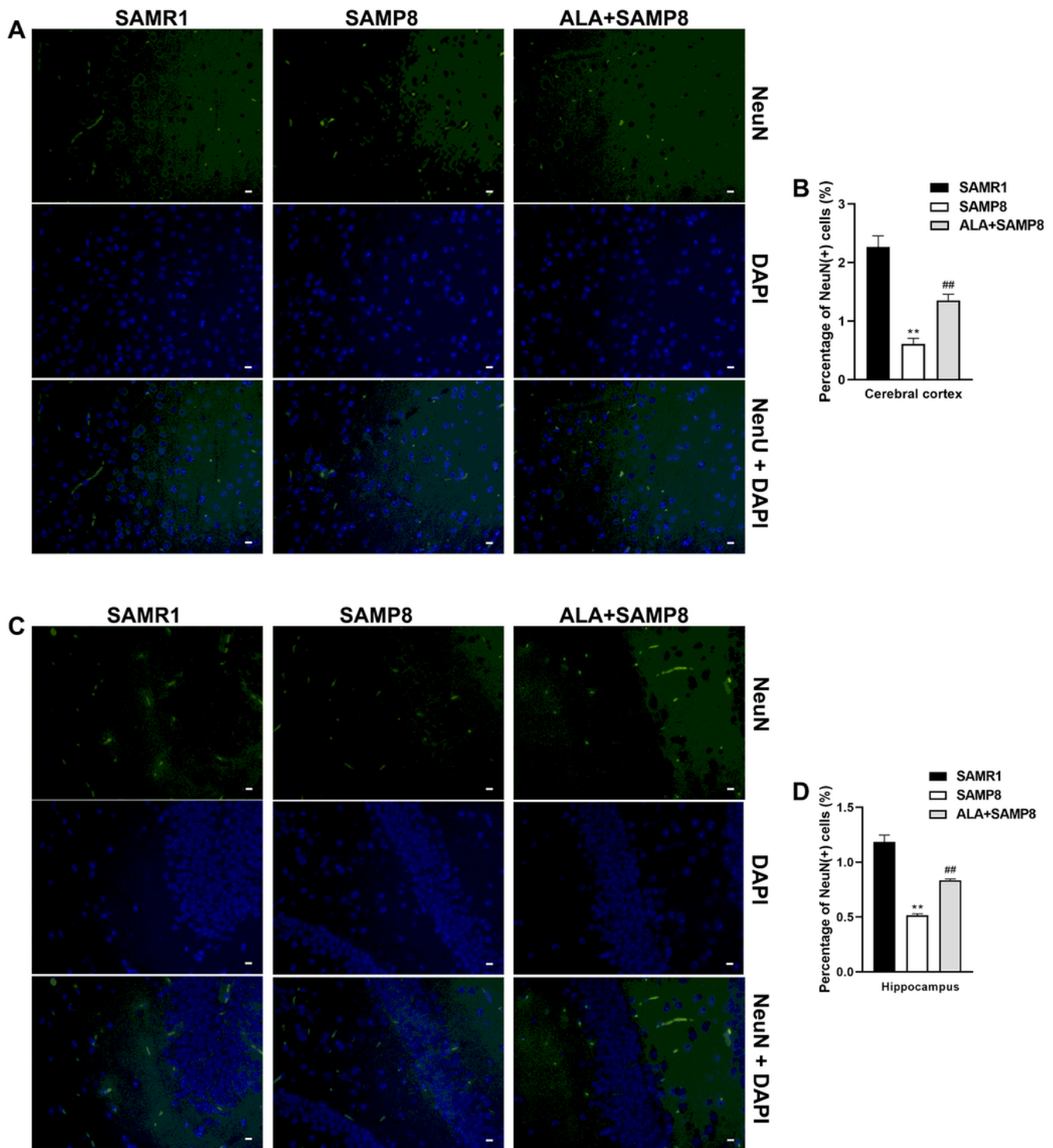


**Figure 4**

Morphological changes of neurons in cerebral cortex and hippocampus of mice under immunofluorescence staining. The neurons (green) in the cerebral cortex (a) and hippocampus (b) of mice were stained (100  $\mu$ m); The percentage of NeuN (+) cells in cerebral cortex (c) and hippocampus (d) of mice were compared (n=2). Data are presented as the mean $\pm$ SEM. \*P<0.05, \*\*P<0.01 vs. SAMR1 mice; #P<0.05, ##P<0.01 vs. SAMP8 mice.

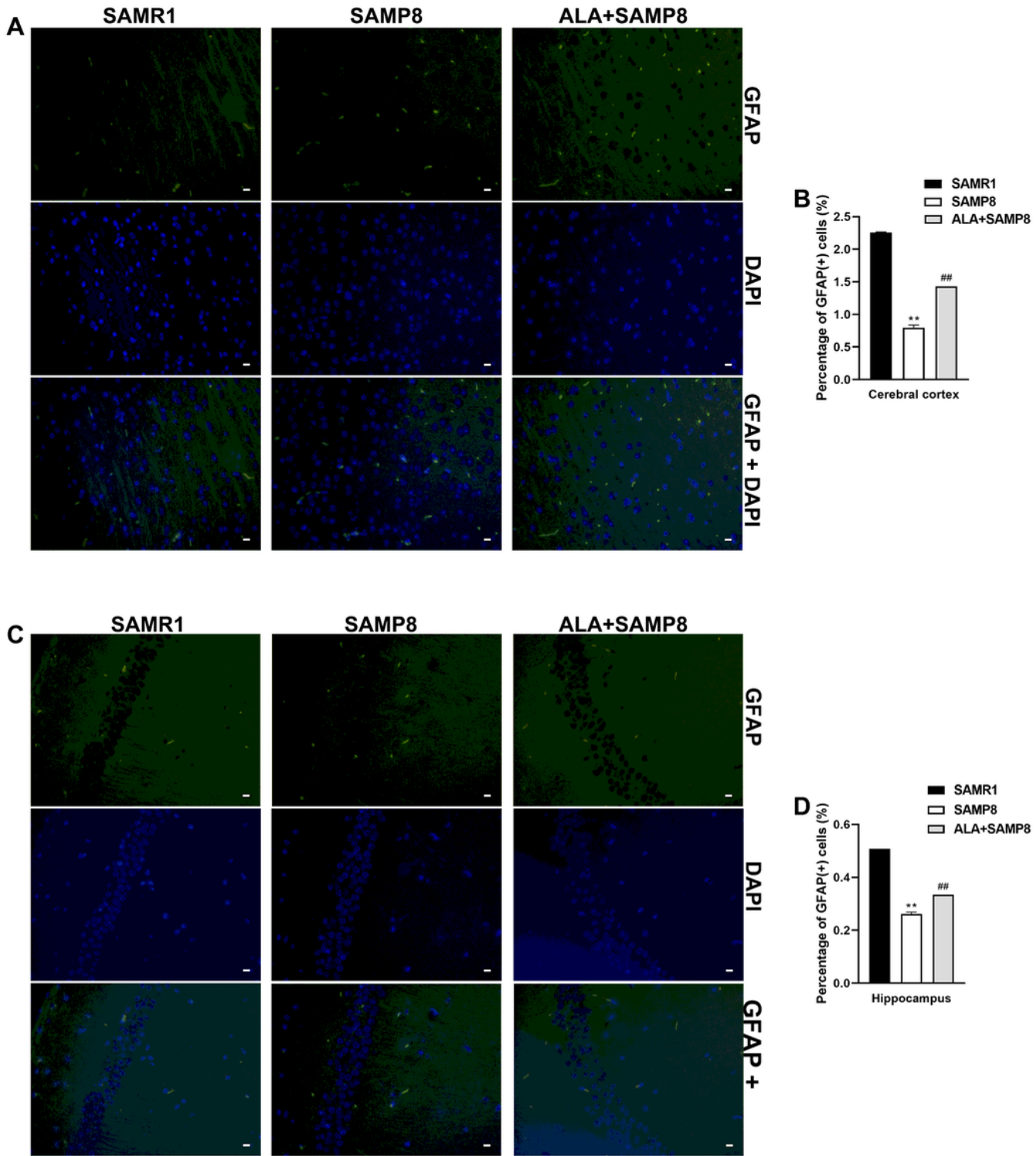


**Figure 5**

Morphological changes of astrocytes in cerebral cortex and hippocampus of mice under immunofluorescence staining. The astrocytes (green) in the cerebral cortex (a) and hippocampus (b) of mice (100  $\mu$ m); The percentage of GFAP (+) cells in cerebral cortex (c) and hippocampus (d) of mice were compared (n=2). Data are presented as the mean  $\pm$  SEM. \*P<0.05, \*\*P<0.01 vs. SAMR1 mice; #P<0.05, ##P<0.01 vs. SAMP8 mice.

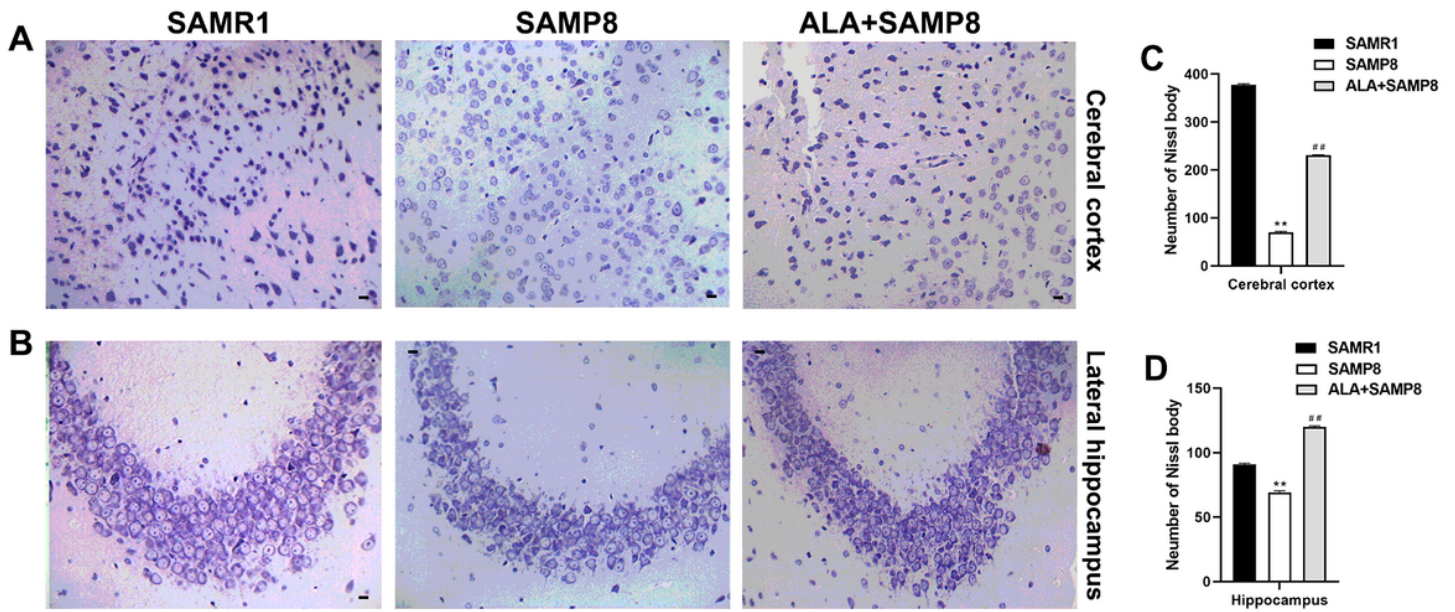


**Figure 6**

Morphological changes of Nissl bodies under Nissl staining The Nissl bodies in the cerebral cortex (a) and hippocampus (b) of mice were stained (100  $\mu\text{m}$ ); The number of Nissl bodies in the cerebral cortex (c) and hippocampus (d) of mice were compared (n=2). Data are presented as the mean $\pm$ SEM. \*P<0.05, \*\*P<0.01 vs. SAMR1 mice; #P<0.05, ##P<0.01 vs. SAMP8 mice.

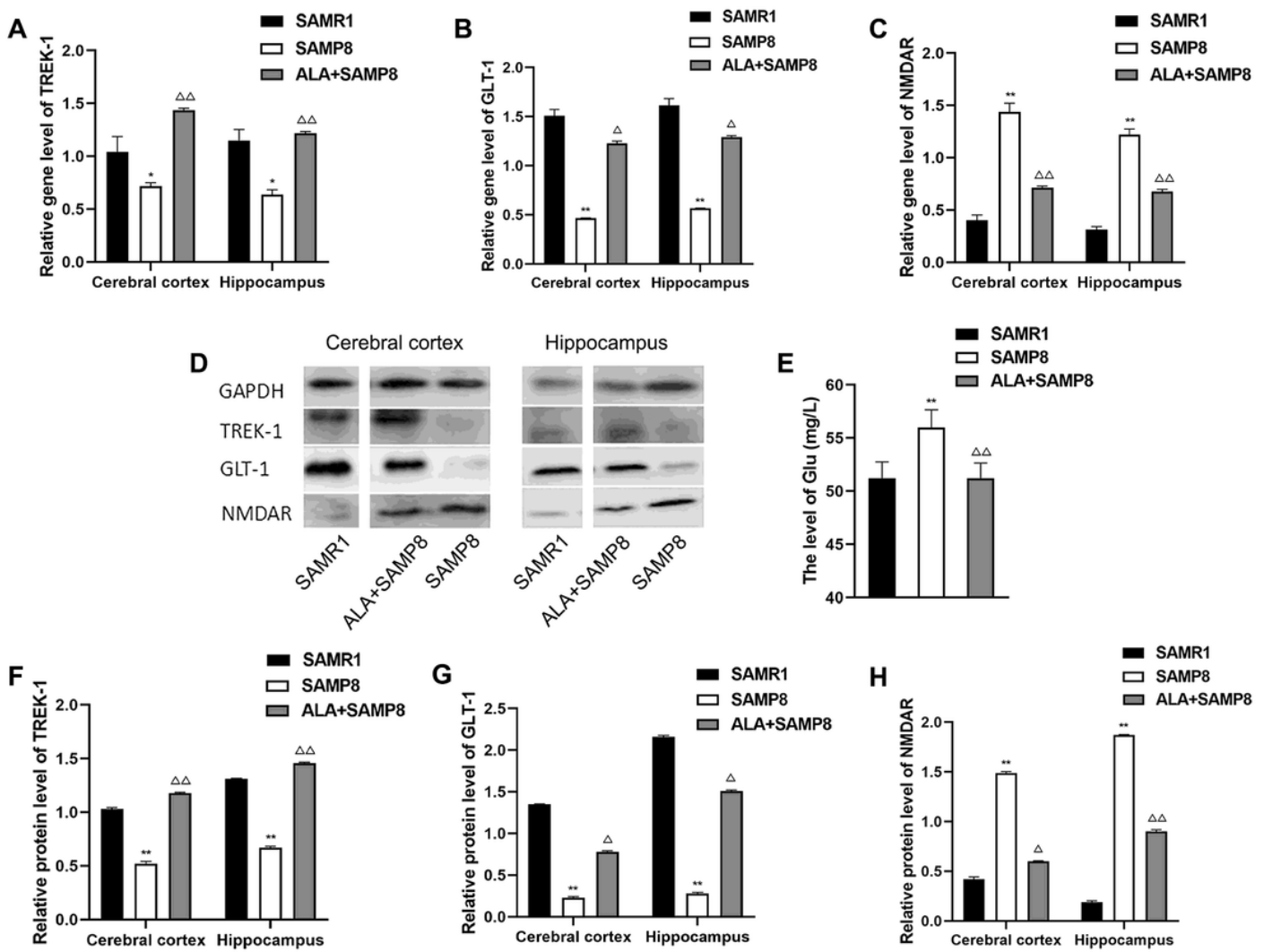


**Figure 7**

Effects of ALA on levels of TREK-1 and Glutamate metabolic pathway in SAMP8 mice. Relative gene expression levels of TREK-1 (a), GLT-1 (b) and NMDAR (c) in the cerebral cortex and hippocampus (n=3); (d) Expression bands of TREK-1, GLT-1, and NMDAR protein in the cerebral cortex and hippocampus; (e) The levels of Glu in the brains of mice were compared. The relative expression levels of TREK-1 (f), GLT-1 (g) and NMDAR (h) proteins in the cerebral cortex and hippocampus of mice (n=3). Data are presented as the mean  $\pm$  SEM. \* $P < 0.05$ , \*\* $P < 0.01$  vs. SAMR1 mice;  $\Delta P < 0.05$ ,  $\Delta\Delta P < 0.01$  vs. SAMP8 mice.